

Bayesian Neural Network Surrogates for Bayesian Optimization of Carbon Capture and Storage Operations

Sofianos Panagiotis Fotias^{a,*}, Vassilis Gaganis^{a,b}

^a*School of Mining and Metallurgical Engineering, National Technical University of Athens, 157 73, Athens, Greece*

^b*Institute of Geoenergy, Foundation for Research and Technology, Chania, 73100, Greece*

Abstract

Carbon Capture and Storage (CCS) stands as a pivotal technology for fostering a sustainable future. The process, which involves injecting supercritical CO₂ into underground formations, a method already widely used for Enhanced Oil Recovery, serves a dual purpose: it not only curbs CO₂ emissions and addresses climate change but also extends the operational lifespan and sustainability of oil fields and platforms, easing the shift toward greener practices. This paper delivers a thorough comparative evaluation of strategies for optimizing decision variables in CCS project development, employing a derivative-free technique known as Bayesian Optimization. In addition to Gaussian Processes, which usually serve as the gold standard in BO, various novel stochastic models were examined and compared within a BO framework. This research investigates the effectiveness of utilizing more exotic stochastic models than GPs for BO in environments where GPs have been shown to underperform, such as in cases with a large number of decision variables or multiple objective functions that are not similarly scaled. By incorporating Net Present Value (NPV) as a key objective function, the proposed framework demonstrates its potential to improve economic viability while ensuring the sustainable deployment of CCS technologies. Ultimately, this study represents the first application in the reservoir engineering industry of the growing body of BO research, specifically in the search for more appropriate stochastic models, highlighting its potential as a preferred method for enhancing sustainability in the energy sector.

Keywords: CCS, Bayesian Optimization, Markov Chain Monte Carlo, Variational inference, Gaussian Process, Reservoir Simulation

1. Introduction

Achieving net-zero greenhouse gas emissions by mid-century necessitates significant investment in near-zero emissions technologies across industries [1]. Carbon Capture, Utilization and Storage (CCUS) is a pivotal strategy in this transition, offering a flexible solution for decarbonizing diverse sectors by capturing CO₂ and sequestering it permanently in geological formations [2, 3]. Viable storage sites, such as deep saline aquifers or depleted hydrocarbon reservoirs

*Corresponding author.

Email address: sfotias@metal.ntua.gr (Sofianos Panagiotis Fotias)

[6, 7, 8, 9, 10, 11], must possess specific geological characteristics including adequate porosity, permeability and robust caprock integrity to ensure secure, long-term containment [4, 5]. Effective CCUS deployment relies on meticulous site characterization and predictive numerical modeling to understand subsurface CO₂ behavior and trapping mechanisms [12, 13, 14].

Numerical reservoir simulations are thus indispensable for evaluating CCS project performance as they simulate the fluid behavior through solving a discretized form of the Darcy equation [15]. In this study, OPM’s open-source Flow software [16], which employs a black-oil model formulation [17] adapted for CO₂ brine systems, is utilized to simulate multi-phase compressible fluid flow and CO₂ trapping. Building on such accurate, albeit computationally intensive, simulation modeling, optimizing the development schedule is crucial for maximizing sequestration potential and economic viability in CCS projects [18, 19]. The primary goal of CCS operational optimization is to maximize CO₂ storage and/or economic returns, often expressed through the Net Present Value (NPV) function, while adhering to technical guidelines, operational constraints and commercial needs [20, 21]. Common strategies involve managing CO₂ injection rates and pressure buildup, often through brine production, with operational limits dictated by factors such as CO₂ breakthrough and maximum bottomhole pressures [22, 23, 24, 25]. Decision variables for CCS operators typically include well placement and time-varying fluid injection/production rates. The resulting objective functions are often case-dependent, computationally expensive to evaluate (requiring full reservoir simulations) and exhibit complex, non-linear behavior, making them black-box functions suitable for multi-objective optimization [26]. While simulators internally handle some constraints (e.g., bottomhole pressures), others, such as preventing CO₂ migration beyond licensed areas or beyond structural traps, must be managed by the optimization process.

The inherent complexity, non-linearity, local optima and numerous constraints in CCS optimization have led researchers to predominantly employ derivative-free optimization approaches [38]. Methods such as Genetic Algorithms (GAs) [27, 29, 30, 32] and Particle Swarm Optimization (PSO) [28, 34, 37], often augmented with heuristics or global sampling strategies like Latin Hypercube Sampling (LHS) [36], have been widely used for tasks like well placement and operational control in CCS and broader reservoir management [31, 35]. While effective for navigating non-smooth objective functions, these methods suffer from data inefficiency, particularly when direct objective function evaluations require computationally expensive, fully implicit reservoir simulations, as in this work.

To mitigate this computational burden without resorting to potentially oversimplified proxy reservoir models, surrogate modeling has emerged as a preferred alternative [39]. Surrogate models are computationally efficient approximations of the true objective function, built from a limited number of accurate simulation runs [40]. Deterministic surrogates, such as radial basis functions, Kriging and multivariate adaptive regression splines, have been investigated for reservoir engineering optimization [42, 43, 44, 45]. However, careful selection of the surrogate strategy is crucial to avoid issues like convergence to non-existent optima [41]. Furthermore, deterministic models, especially those with many parameters like conventional neural networks, are prone to overfitting [46] and critically, cannot effectively quantify predictive uncertainty [47, 48]. This lack of uncertainty quantification is particularly detrimental in data-scarce CCS optimization. Bayesian Optimization (BO) addresses these limitations by employing stochastic surrogate models [49]. These models provide a robust mathematical framework to quantify both aleatoric

uncertainty (e.g., from simulation noise or discrepancies between the model and reality) and epistemic uncertainty (stemming from a lack of data) [50, 51]. BO iteratively constructs and updates these stochastic surrogates, most commonly Gaussian Processes (GPs) [52], to efficiently guide the search for the global optimum, making it well-suited for CCS optimization.

BO, typically utilizing GP surrogates, has been successfully employed within reservoir engineering for diverse challenges. These include well placement optimization [53], field development planning under geological uncertainty to maximize NPV [54], optimizing gas/surfactant injection cycles in WAG schemes [59], refining deviated well trajectories [60] and optimizing fracturing designs [61]. Innovative BO methodologies such as trust region BO and sparse-axis aligned subspaces BO (SAASBO) have also been introduced [55, 56, 57, 58, 84]. General advancements in BO research, extensively reviewed by Garnett et al. (2023) [68], have focused on areas like novel acquisition functions [62], expressive kernel designs [63, 64], gradient-informed BO [65], multi-objective optimization [66] and extensions to discrete spaces [67]. Our own recent work contributed a permutation invariant kernel for CCS well placement optimization [69]. Despite these advancements and the successes of GP-based BO, the exploration of alternative stochastic surrogate models, particularly for the complex demands of CCS optimization, remains a pertinent research direction.

While Bayesian approaches, including Markov Chain Monte Carlo (MCMC) (2.2.2) and specialized algorithms like NAB [72, 73], are employed in reservoir engineering for tasks such as history matching and uncertainty propagation through development stages [71, 74, 75, 76, 77, 78, 70], our focus is distinct. This study investigates Bayesian Neural Networks (BNNs) [79] as alternative surrogate models to GPs within the BO framework, specifically for optimizing CCS operational decisions. MCMC techniques are utilized herein to sample from the BNN posterior over surrogate model parameters, not for history matching or uncertainty propagation across project phases.

BNNs offer potential advantages over traditional GPs for complex optimization tasks. They can model dynamic, non-stationary behavior and learn latent similarity measures via representation learning, features particularly valuable for high-dimensional inputs and multi-output objectives common in CCS [80]. The recent development of Monte Carlo-based acquisition functions, which only require posterior samples from the surrogate, further facilitates the use of non-GP models like BNNs that may not have closed-form predictive distributions [81]. Therefore, this paper presents a comparative evaluation of various BNN-based surrogates against GPs for Bayesian Optimization of CCS operations, building upon the framework and code contributions of Li et al. (2023) [80]. The primary contributions of this work include an extension of this framework to incorporate additional BNN surrogate models (detailed in Section 2) and a novel application and comparative assessment of these advanced surrogate modeling techniques for BO in a reservoir engineering context, specifically for CCS.

The rest of the paper is organized as follows. Section 2 provides an overview of the stochastic surrogate models implemented. Section 3 details the CCS case studies used for optimization. Section 4 presents and analyzes the optimization results. Section 5 offers a broader discussion on the methodology, its application and performance. Finally, conclusions are drawn in Section 6 based on the findings presented throughout the study.

2. Methods

2.1. Gaussian Processes

Gaussian Processes (GPs) are the standard surrogate models in Bayesian Optimization (BO) due to their ease of implementation, fast training and inherent ability to quantify epistemic uncertainty through their kernel functions [83, 49]. A GP defines a probability distribution over functions, characterized by a mean function, specifying the prior expected value at any input and a covariance (or kernel) function, quantifying the similarity and correlation between function values at different input points [87, 83]. The kernel essentially encodes prior beliefs about the function’s smoothness and behavior; in this work, the flexible Matérn kernel is employed due to its generality [88]. For comprehensive theoretical details and visual explanations, readers are referred to Rasmussen and Williams (2006) [83] and popular expositions [85, 86]

Given a set of observations obtained by evaluating the expensive black-box function, the GP prior is updated to a posterior distribution over functions. This posterior provides a predictive mean and variance for any new potential candidate test point in the feasible space. These predictive distributions are then utilized by the acquisition functions (2.4) to decide where to sample next.

2.2. Bayesian Neural Networks

While GPs are powerful, their performance can be limited by the choice of stationary kernels in complex, high-dimensional, or multi-objective scenarios common in CCS optimization. BNNs offer a flexible alternative by placing prior distributions over the weights and biases of a neural network architecture [91, 92, 93, 94, 80]. Instead of learning point estimates for parameters as in standard ANNs, BNNs aim to infer a posterior distribution over these parameters given the observed data. This allows BNNs to inherently quantify predictive uncertainty: predictions from a BNN are obtained by marginalizing over this posterior distribution, effectively averaging over an ensemble of ANNs [95, 96]. However, the true posterior is generally intractable to compute directly due to the high-dimensional, non-convex nature of the parameter space and the difficulty in evaluating the evidence term [98]. Consequently, approximate inference techniques are required. The main approaches include Variational Inference (VI) and Markov Chain Monte Carlo (MCMC) sampling methods.

2.2.1. Variational Inference

Variational Inference (VI) approximates the intractable true posterior with a simpler, tractable distribution (e.g., a factorized Gaussian) [101]. The goal is to minimize the Kullback-Leibler (KL) divergence between the intractable posterior and the tractable one, which is equivalent to maximizing the Evidence Lower Bound (ELBO) [102, 103]. Stochastic Variational Inference (SVI) is a common optimization technique for this [104], often employing approximations like diagonal covariance matrices for scalability [105, 106, 107]. Further details on VI and ELBO maximization can be found in works like [108, 109, 110, 111, 112].

2.2.2. Markov Chain Monte Carlo

As an alternative to approximating the posterior directly, sampling methods aim to draw samples from the BNN posterior. These samples are then used to estimate the predictive distribution for BO [99, 100]. While basic methods like rejection sampling [113] have limitations in high dimensions, MCMC algorithms such as Metropolis-Hastings construct a Markov chain whose stationary distribution is the target posterior [114, 115, 116].

For complex, high-dimensional posteriors common in BNNs, Hamiltonian Monte Carlo (HMC) and its variants, like the No-U-Turn Sampler (NUTS) [120], are often more efficient [118, 117]. HMC introduces auxiliary momentum variables and leverages Hamiltonian dynamics to propose distant, high-acceptance-probability samples, effectively navigating the geometry of the typical set of the distribution. This is particularly advantageous in exploring regions of high curvature where simpler random-walk MCMC methods struggle. HMC methods typically require gradient information of the log-posterior and careful tuning of parameters, often involving symplectic integrators to maintain numerical stability [119, 121, 122].

2.3. Approximate Bayesian

Beyond VI and MCMC, several computationally less intensive 'approximate Bayesian' techniques are used to obtain uncertainty estimates from neural networks, making them suitable for BO surrogates.

2.3.1. MC dropout

Dropout [123] is a method initially developed for regularization of deep networks. The key idea is to randomly drop units from each layer during training thereby preventing units from co-adapting. MC dropout [124] is a method that builds on this idea by keeping the dropout probabilities when making predictions on new inputs. For each input, multiple outputs are evaluated and a mean and variance can be easily derived from this sampling process. MC Dropout has been shown to approximate a specific form of VI under certain conditions [124]. This method is very convenient and straightforward to implement.

2.3.2. Deep Ensembles

Deep Ensembles [125] is another straightforward and easily implemented method. This method works by training multiple point estimate neural networks, each one on another subset of the training dataset with a different random seed for the initial hyperparameters. The posterior is approximated with a distribution parameterized as the sum of multiple Dirac delta functions. These methods provide a good predictive uncertainty estimate [126].

2.3.3. Infinite width Neural Networks

A deep neural network in the limit of infinite width was shown to be equivalent to a GP [127, 128] using the Central Limit Theorem. This can be extended for not only a single network but for any number of additional hidden layers as well [129]. The kernel function of this GP is complex and can be derived from the architecture of the network and its computation is deterministic and differentiable.

2.3.4. Deep Kernel Learning

Deep Kernel Learning (DKL) [130] is a hybrid method where a neural network transforms the input features into a new representation, upon which a standard GP kernel is then applied. This allows the model to learn complex, non-stationary feature mappings before leveraging the probabilistic framework of GPs.

2.4. Acquisition functions

The BO loop iteratively selects new points for evaluation using an acquisition function, which leverages the surrogate model's predictive mean and variance to balance exploration (sampling in uncertain regions) and exploitation (sampling near known good values). For single-objective optimization, a common choice is Expected Improvement (EI). EI quantifies the expected amount by which a new candidate point will improve upon the best objective value observed so far. When a closed-form posterior from the surrogate is unavailable (as with BNNs), a Monte Carlo approximation (MC-EI) is used where posterior samples of the surrogate model parameters are drawn, predictions are made at candidate points and the expected improvement is averaged over these samples. The point maximizing this MC-EI is chosen for the next evaluation .

For multi-objective optimization problems, as encountered in this study, EI is extended to Expected Hypervolume Improvement (EHVI). EHVI measures the expected increase in the hypervolume of the objective space dominated by the current Pareto front of non-dominated solutions, given a new set of candidate points. Similar to MC-EI, Monte Carlo EHVI (MC-EHVI) is computed by averaging the hypervolume improvement over predictions from posterior samples of the surrogate model. The batch of candidate points that maximizes MC-EHVI is then selected for evaluation. This approach guides the search towards solutions that broadly improve across all objectives by expanding the dominated region of the Pareto front

3. Problem description

3.1. The reservoir system

This study extends our previous work [69], which examined the carbon sequestration potential of a deep, highly permeable synthetic aquifer. As illustrated in Figure 1 (generated using ResInsight, an open-source tool for 3D visualization, curve plotting and post-processing of reservoir models and simulations), the aquifer exhibits an inclined geometry reminiscent of an anticline. It spans a large horizontal area and is composed of four sedimentary layers, each characterized by different average permeability values. The formation is tightly sealed by shale, with no evident faulting or fracturing and it maintains a salinity of approximately 65,000 ppm. The temperature profile of the aquifer adheres to expected thermal gradients at its depth, as detailed in Table 1. Due to its high permeability, the pressure distribution within the aquifer aligns with the pressure gradient and remains isotropic in the x - y plane. However, the aquifer is slightly overpressurized, which necessitates the simultaneous extraction of brine during CCS operations. This approach is critical for postponing the attainment of the upper pressure safety limit of 9,000 psi mandated by technical and safety protocols. The significance of this strategy is further underscored by the no-flow boundary conditions imposed at the aquifer's lateral bounds in the simulation model [131].

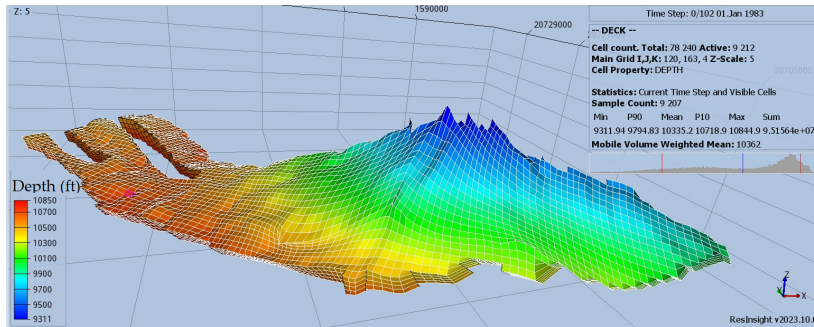


Figure 1: Aquifer depth (z axis is scaled)

Table 1: Aquifer static properties (average values)

Parameter	Value	Units
Pressure (P)	5,000	Psi
Temperature (T)	200	$^{\circ}F$
Porosity (ϕ)	0.25	
Depth (D)	10,180	ft
Permeability (k)	300	mD
Bulk volume (V)	$2.4 \cdot 10^{11}$	scf
Water in place	$1.7 \cdot 10^9$	STB

In our previous work, BO was used with a GP surrogate model to optimize well placement of 3 injectors and 8 producers. Exploiting the symmetry of injector and producer locations under the group control policies, a permutation invariant kernel was developed that rapidly expedited the optimization. The objective function selected was the total CO_2 sequestered mass based on predefined target injection and production rates. The optimal configuration is seen in Figure 2.

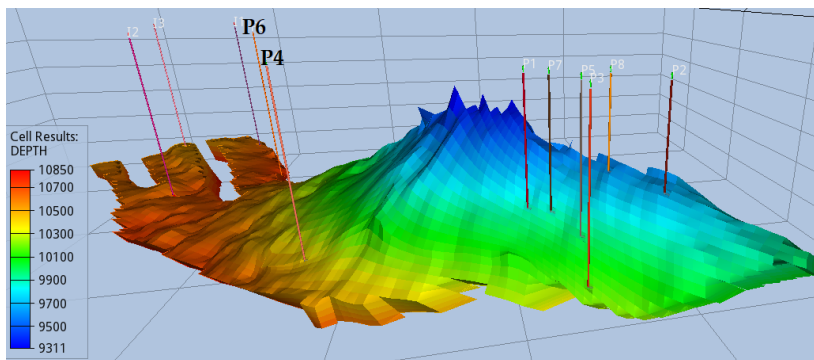


Figure 2: Optimal well placements

All injectors are placed at the bottom of the reservoir, at left side of Figure 2. A cluster of 6 producers has been strategically placed at the opposite side of the aquifer as far away as possible

from the injectors with the exception of two producers, highlighted in the figure, placed closer to the injectors for pressure maintenance. This specific placement and the predefined scheduling will be referred to throughout this work as the "placement optimum" configuration for easy reference. Note that the number of producers had been deliberately exaggerated to demonstrate the value of the modified kernel function developed for the GP surrogate [69].

Building upon this, the attention now turns to optimizing the injection and production rates over the envisaged injection period. Based on the results of the optimal configuration achieved, the CO₂ injection rate profile can be seen in the blue line of Figure 3. In this work, two approaches will be utilized for optimization, one with a single objective function and a few decision variables (≈ 10) and a multi-objective optimization problem with many decision variables (≈ 1000). The finite width stochastic BNNs utilized have three hidden layers of 100 fully connected neurons each. The models are named as seen in Table 2.

Table 2: Model names

Model Name	Model Description
GP	Gaussian Process with Matern kernel (Section 2.1)
SVI	Stochastic Variational Inference (Section 2.2.1)
MCMC	Hamiltonian Monte Carlo (Section 2.2.2)
NUTS	Hamiltonian Monte Carlo with No-U-Turn Sampler (section 2.2.2)
IBNN	Infinite Width Bayesian Neural Network (Section 2.3.3)
Ensemble	Deep Ensembles (Section 2.3.2)
Dropout	MC dropout (Section 2.3.1)
DKL	Deep Kernel Learning (Section 2.3.4)

The BO framework is built upon Li's work [80] that utilizes Gpytorch [132] and Botorch [81] for the models and BO with the addition of Pyro [133] for the NUTS and SVI models. The framework consists of selecting 15 initial points for evaluation and subsequently performing 15 BO iterations for each model, selecting the 4 best candidate points to be evaluated and updating the training dataset each time.

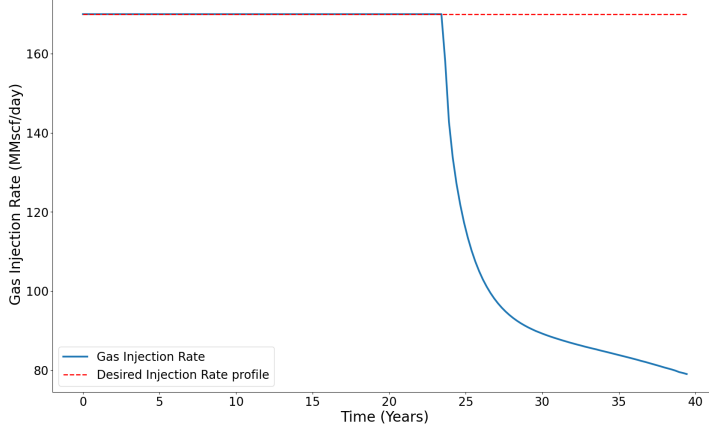


Figure 3: Placement optimum configuration injection performance

3.2. Case study 1

In the placement optimum case, while the target injection rate of 170 MMscf/day is managed to remain constant for 23 years, it expectedly and rapidly drops off after this period. Due to gas breakthrough, producers operate under a reduced rate than the constant predefined target one, resulting in a pressure increase and a subsequent drop in gas injection rate due to the max bottomhole pressure constraint. In this case study, the group control policy of the injection wells is necessary since ideally, a constant total sequestration rate would be essential to honor the operator's contracts to the emitters, therefore it needs to remain constant and it has been kept at the same value of 170 MMscf/day. However in search for more operational decision variables and increased flexibility, the group control policy has been removed from the producers. By making them independent, it is hoped that BO can find target production rates for each well independently so as the target injection rate is honored throughout the project's lifespan without unnecessary CO₂ recycling. This is a classic single objective optimization problem, formulated in Eq. 1.

$$\begin{aligned} \text{maximize}_{\mathbf{x}} \quad & f(\mathbf{x}) = 1 / \left[\sum_t \left| Q_{CO_2}^{\text{inj}}(t) - Q_{CO_2}^{\text{inj}}(t-1) - Q_{CO_2}^{\text{prod}}(t) \right| \cdot k(t) \right] \\ \text{subject to} \quad & g_i(\mathbf{x}) \leq 0, \quad i = 1, 2, \dots, m \end{aligned} \quad (1)$$

where $f(\mathbf{x})$ corresponds to the change in actual sequestration rate of the whole field $Q_{CO_2}^{\text{inj}}$ per timestep minus a correction $Q_{CO_2}^{\text{prod}}$ to penalize CO₂ recycling. The term $k(t) \propto 1/t$ is utilized to penalize harder the injection rate drop at the initial stages of the project as opposed to the latter ones. This objective is sampled by simulation runs. Furthermore \mathbf{x} are the decision variables, in this case the target production rate of each producer and the maximum breakthrough allowed. The constraints $g_i(\mathbf{x}) \leq 0$, are the bounds of the decision variables and the bottomhole pressure constraints which are handled by the simulator and thus need not be introduced directly in the optimization formulation. Decision variables and constraints can be seen in detail in Table 3

Table 3: Decision variables for first variation of Case study 1

# variables	Variable type	Range
8	(Target) Production Rate (Water)	≤ 100 Mstb/day
8	(Constraint) Max Production Rate (CO ₂)	≤ 8 MMscf/day

Since in practice, BO managed to easily converge to an optimal scenario where injection rate is kept constant throughout the development, a second variation of this case is also examined by trying to increase the injection rate, using it as an extra decision variable rather than fixing it at 170 MMscf/day. The decision variables of the second variation of Case study 1 can be seen in Table 4.

Table 4: Decision variables for second variation of Case study 1

# variables	Variable type	Range
1	(Target) Injection Rate (CO ₂)	170 – 200 MMscf/day
8	(Target) Production Rate (Water)	≤ 100 Mstb/day
8	(Constraint) Max Production Rate (CO ₂)	≤ 8 MMscf/day

This variation was handled as a multi-objective optimization case with the first objective being the same as in the first variation and the second being the total sequestration, for the optimizer to be guided towards larger injection rates.

$$f_2(\mathbf{x}) = \sum_t (Q_{CO_2}^{inj}(t) - Q_{CO_2}^{prod}(t))$$

Although a target rate limit of 100 Mstb/day for a producer might be way over the maximum capacity of what a well can handle, reservoir simulators enforce physical constraints (such as bottomhole pressure limits), so any target rate exceeding feasible bounds defaults to the same practical outcome. In other words, selecting an infeasibly large rate yields no advantage and becomes a “trivial solution”. Importantly, different optimization methods tested here converge to different optimal points rather than uniformly exploiting such trivial upper limits. This confirms that the optimization procedure identifies genuinely distinct, physically valid and non-trivial solutions.

3.3. Case study 2

In the second case, the cluster of the 6 producers in the placement optimum case, was replaced by a single one seen in Figure 4, to emulate operations capital expenditure (CAPEX) reduction goals.

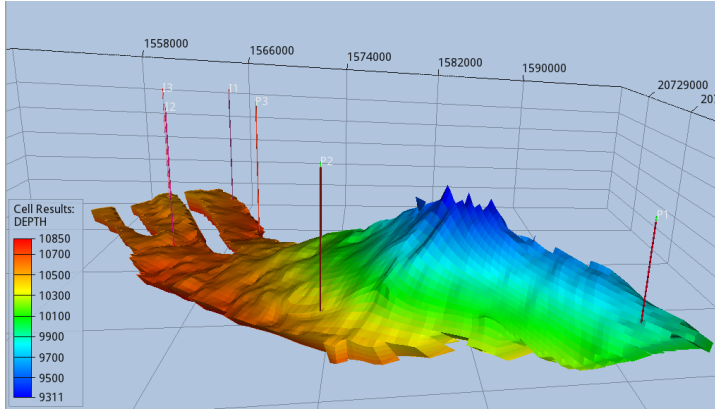


Figure 4: reduced placement optimum

Although it is not typical to budget the drilling of 6 wells for pressure maintenance as each one's cost is in the range of tens of millions of dollars, it needs to be noted that most producers in the cluster could function as lateral extensions of a few multi-segment horizontal wells thereby reducing the costs. Regardless, by performing this aggregation, the total amount of CO₂ sequestered drops significantly as seen in Figure 5. This case will be referred to as the "reduced placement optimum" one.

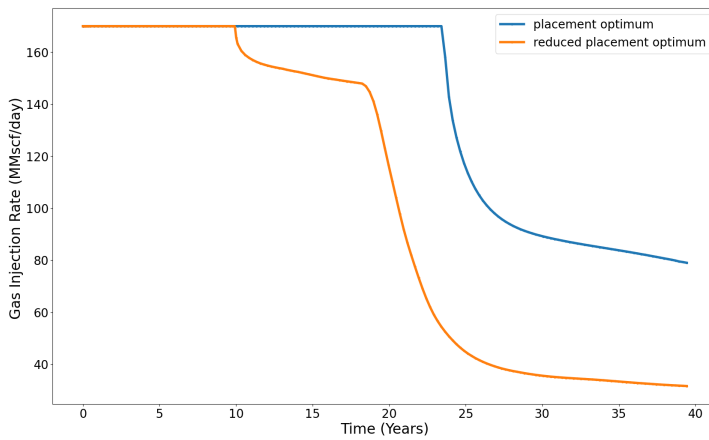


Figure 5: Gas injection rate profile

Similar to the previous case study, the group control policy of the three producers retained is removed. Their target rate as well as their allowable breakthrough rate is adjusted by the optimizer on a 90 days basis. Since the designed project duration is 40 years, the number of decision variables increased rapidly. Furthermore, a single decision variable is used for the target injection rate, slightly tunable from the base value of 170 MMscf/day. The decision variables are shown in Table 5.

Table 5: Decision variables for Case study 2

# variables	Variable type	Range
1	(Target) Injection Rate (CO ₂)	150 – 190 MMscf/day
480	(Target) Production Rate (Water)	≤ 100 Mstb/day
480	Constraint) Max Production Rate (CO ₂)	≤ 8 MMscf/day

In this optimization case, four objective functions were utilized. The goal is for the BO to optimize the reduced placement optimum case's variables to be as close as possible to the placement optimum one's in each objective function necessary for a CCS project. The four objective functions are shown below in Eq. 2

$$\begin{aligned}
\text{maximize}_{\mathbf{x}} \quad & f_1(\mathbf{x}) = \frac{M_{CO_2}^{\text{residual}} + M_{CO_2}^{\text{dissolved}}}{M_{CO_2}^{\text{mobile}}} \\
\text{maximize}_{\mathbf{x}} \quad & f_2(\mathbf{x}) = \sum_t (Q_{CO_2}^{\text{inj}}(t) - Q_{CO_2}^{\text{prod}}(t)) \\
\text{maximize}_{\mathbf{x}} \quad & f_3(\mathbf{x}) = 1 / \left[\sum_t |Q_{CO_2}^{\text{inj}}(t) - Q_{CO_2}^{\text{inj}}(t-1)| \cdot k(t) \right] \\
\text{maximize}_{\mathbf{x}} \quad & f_4(\mathbf{x}) = \sum_t \Delta t_n (C_{\text{storage}} \cdot Q_{CO_2}^{\text{stored}} - C_{\text{injection}} \cdot Q_{CO_2}^{\text{inj}} - C_{\text{production}} \cdot Q_{\text{brine}}) / (1+r)^{t/365} \\
\text{subject to} \quad & g_i(\mathbf{x}) \leq 0, \quad i = 1, 2, \dots, m
\end{aligned} \tag{2}$$

The first objective aims at maximizing the desired trapping mechanisms like solubility of CO₂ in brine and residual which is calculated based on the amount of immovable CO₂ left as the plume moves through the aquifer. The second one is the same as the one used in the second variation of the first case study. The third is the same as the first case study's first variation, without the term penalizing CO₂ recycling as this has now been indirectly introduced to the fourth objective which represents the project Net Present Value (NPV). Of course, approximating the NPV of a CCS project involves a lot of uncertainty since there are not many in operation worldwide yet. Various simplifications have been made in order to use this functional form of the NPV. Costs associated with recasing wells or even drilling new ones have not been dealt with despite potentially being substantial [134]. The cost of injecting CO₂ $C_{\text{injection}}$ has thus been placed at a moderate 6.2 € per tonne injected. The profit of storing emissions C_{storage} is estimated at around 30 € per tonne of CO₂. This is an indicative expected value defined by IEA [135] but it is based on the assumption that it will be a closed contract between the emitter and the CCS operator and not be purchased on the spot market. In fact, due to the fast changing environment of regulations regarding CO₂ emissions, there is a lot of uncertainty surrounding this price in general. Finally the cost of producing and treating brine $C_{\text{production}}$ was set at 2.7 € per tonne [44, 136]. The annual discount rate of the NPV was set at $r = 1.42\%$. This objective function is not meant to provide an exact measure of the profitability of the CCS project. It doesn't account for inflation, initial investment and operational expenses, it is rather meant to serve as a counterweight to extreme brine production and CO₂ breakthrough which hinders profitability.

4. Results

4.1. Case study 1

4.1.1. Variation 1

To start things off, the first variation of Case study 1 is presented. The optimum sequestration rate from the application of BO to each model is shown in Figure 6 along with the placement optimum case to facilitate the comparison. As already mentioned, the optimization has been able to maintain the injection rate at the target value throughout the lifespan of the project, therefore the sequestration rate is shown instead, i.e. injected minus produced CO₂, for the comparison to be meaningful. Since breakthrough inevitably occurs, the expectation is for the models to be able to keep this sequestration rate constant for as long as possible and as close as possible to the target value. The drop off in the sequestration rate, needs to be delayed and definitely not be as steep as in the placement optimum case.

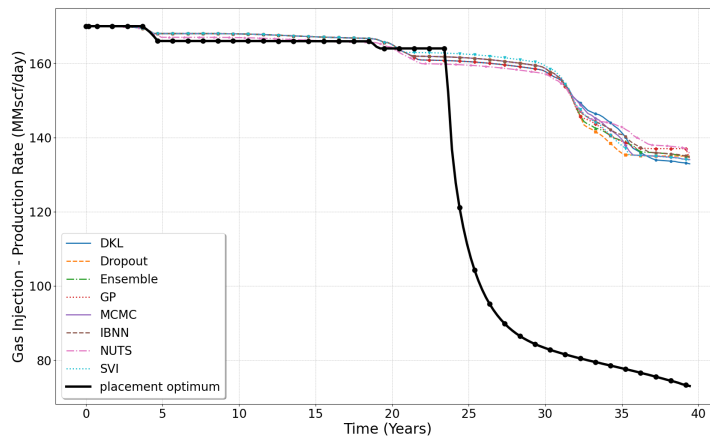


Figure 6: Sequestration rate

The results in Figure 6 indicate that, compared to the benchmark placement optimum case, the solutions proposed by the optimizer do indeed fix the aforementioned issues. In the benchmark case, the sequestration rate drop occurs right after 23 operational years. In comparison, most optimized solutions don't experience this drop up until a decade later, at 31-32 years. All models were able to find the optimal solutions that manages to keep the sequestration rate above 75% of the initial target even as late as the end of the operation, in contrast to the placement optimum, where the sequestration rate dropped to more than 50% by the end of the operation. Notably, all models were able to eventually sequester around 2.3 Tscf of CO₂ out of 2.45 theoretically possible as opposed to the placement optimum case where 1.9 Tscf were sequestered. In Figure 7 the maximum objective function value derived per model is plotted to demonstrate the evolution across sampled values in subsequent BO iterations.

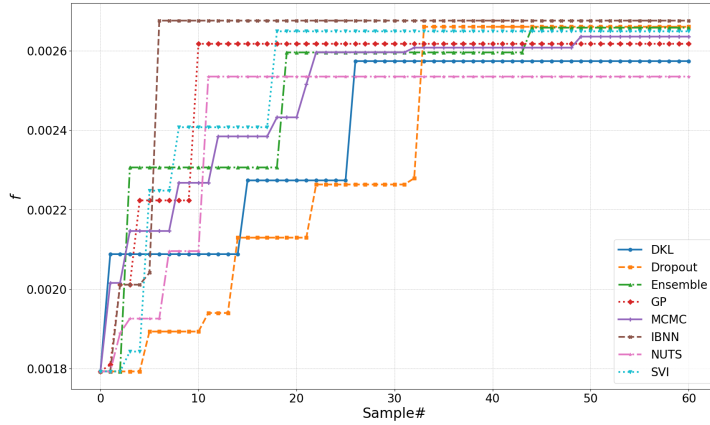


Figure 7: Maximum objective function value vs iteration number

For example, IBNN found improvements over the first two BO iterations but was unable to further improve its predictions. This is probably a result of the value found being near the global optimum one rather than an inability of BO in general. On the other hand, Dropout was consistently finding points with better evaluations and eventually converged close to the optimum but, it was the slowest to reach its best evaluation and finished in second place. The third highest value was found by the Ensemble model. Like IBNN, GP also didn't achieve further improvements after the third iteration and its max value is lower than the highest one observed. This is unexpected considering that GPs are models that usually perform exceptionally well in spaces of low dimensions. The MCMC model also managed to improve throughout BO iterations and eventually converged close to the maximum. The DKL model performed slightly worse compared to the others. As for the Pyro models, NUTS achieved most of its improvement at the first iterations but was unable to improve after, ranking it last in terms of max value produced. On the other hand, SVI consistently improved fast and was able to approach to the overall max value much better.

4.1.2. Variation 2

In the second variation, results for sequestration are way more varied as depicted in Figure 8 which is the plot of the sequestration rate of the best solutions of all models according to the second objective. In this variation models were free to explore a bigger rate of injection target rate, but most of them found no advantage doing so despite utilizing an objective directly related to total sequestration.

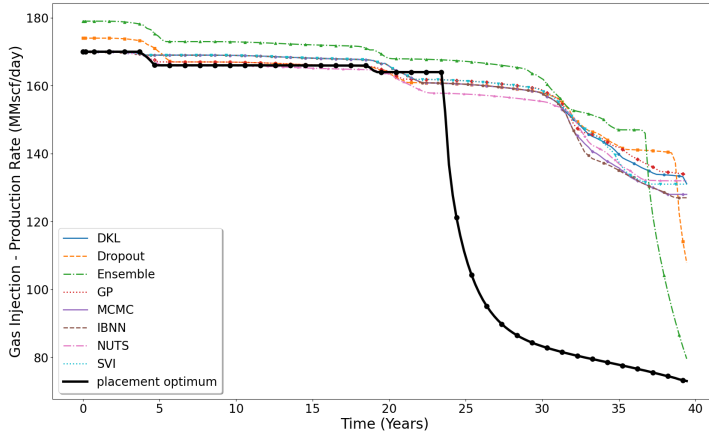


Figure 8: Sequestration rate

The placement optimum case is still the first one to have its sequestration rate drop off rapidly. All models besides Ensemble and Dropout converged to a solution that produced a similar sequestration profile as variation one. Ensemble and Dropout however, explored more towards solutions of higher injection rate and while in both cases sequestration rate didn't drop off until after 37 years of operation, the pronounced and steep drop off impacted the hypervolume of the optimal solution, making both solutions suboptimal.

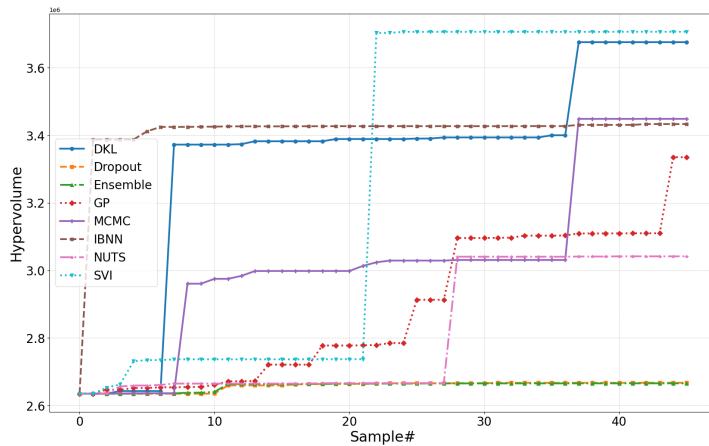


Figure 9: Hypervolume vs iteration number

Figure 9 presents the evolution of the hypervolume for all surrogate models. The Ensemble and Dropout models have slightly improved only at early BO iterations but due to their exploring different optimal solutions, they finished last in terms of hypervolume maximization. In contrast and similarly to the first variation, IBNN improved significantly at an early BO iteration and then struggled for further improvements. NUTS improved slightly at first and significantly only once at a later iteration. MCMC and GP improved steadily throughout the BO iterations. SVI

achieved the best result overall, closely followed by DKL.

4.2. Case study 2

In this case study, the optimization problem involves a high number of variables and four competing objective functions. Notably, the first and third objectives are negatively correlated with the second and fourth. Specifically, the first objective evaluates the safety of CO₂ sequestration, while the third measures the decline in injection rate, primarily due to overpressurization. These objectives tend to be maximized when the injection rate is low. In contrast, the second and fourth objectives assess total sequestration capacity and economic profitability, both of which benefit from higher injection rates. Given the increased complexity of this optimization problem, a more computationally intensive environment with greater CPU and GPU resources was required. Consequently, instead of running a single trial with 12 BO iterations and 5 samples per iteration, as done in Case Study 1, this study was expanded to include 8 trials. Each trial consisted of 120 BO iterations, while the number of samples per iteration remained at 5.

Firstly, the results for the four objectives in both the reduced placement optimum and placement optimum benchmark cases are presented in Table 6. As a reminder, both cases were run with a fixed target injection rate of 170 MMscf/day.

Table 6: Objective function results on benchmark cases

	f_1	f_2 (Tscf)	f_3	f_4 (Billion €)
placement optimum	0.3885	1.9292	0.0012	1.4673
reduced placement optimum	0.4831	1.4062	0.0006	1.1511

When the number of producers is reduced, the last three objective function values decline significantly. For instance, the NPV of the project decreases by 300 million €, a loss that far exceeds the cost savings from drilling fewer producers. Additionally, total CO₂ sequestration drops substantially, shortening the overall project lifespan—a trend already illustrated in Figure 4. The only exception is the first objective function, which increases as expected. With an early decline in injection rate and a corresponding rise in pressure, the CO₂ plume becomes immobile more quickly, leading to a higher proportion of dissolution relative to newly injected CO₂.

As previously mentioned, this is a multi-objective optimization problem with no single globally optimal solution. Therefore, to compare the benchmark cases with the optimized ones, the best values are presented for each individual objective optimization. Table 7 displays the solutions from each model that maximized the first objective. Following the same approach, Tables 8, 9 and 10 present the best solutions corresponding to the second, third and fourth objectives, respectively.

Table 7: Results on the optimal cases according to the first objective function

	f_1	f_2 (Tscf)	f_3	f_4 (Billion €)
DKL	0.5904	0.5625	0.0012	0.5263
Dropout	0.6063	0.4986	0.0009	0.4761
Ensemble	0.5896	0.5503	1.00	0.5150
GP	0.5854	0.5835	0.0011	0.5446
MCMC	0.6098	0.4875	0.0008	0.4671
IBNN	0.6123	0.4742	0.0012	0.4536
NUTS	0.6123	0.4576	1.00	0.4378
SVI	0.6151	0.4652	0.0010	0.4465

Compared to the benchmark cases, all models achieved significantly higher values for the first objective (Table 7), while the values for the other three objectives were considerably lower. This suggests that these solutions correspond to scenarios where the injection rate was initially average, but brine production remained minimal. As a result, pressure builds up rapidly, causing the injection rate to decline quickly. This leads to the CO₂ plume becoming immobile, which is interpreted as trapped by the OPM simulator. An exception to this trend is observed in the Ensemble and NUTS models, where the third objective reaches its maximum possible value of 1. However, if the injection rate were maintained constant over the entire 40-year period, much higher values for both NPV and total sequestration would be expected. The only plausible explanation for this outcome is that, in these cases, the injection rate remains low, the production rate is high and the recycling constraint is significantly relaxed.

Table 8: Results on the optimal cases according to the second objective function

	f_1	f_2 (Tscf)	f_3	f_4 (Billion €)
DKL	0.4594	1.7609	0.0010	1.3391
Dropout	0.4591	1.7583	0.0016	1.3373
Ensemble	0.4677	1.7590	0.0004	1.3634
GP	0.4584	1.7666	0.0016	1.3435
MCMC	0.4596	1.7583	0.0012	1.3374
IBNN	0.4583	1.7608	0.0013	1.3370
NUTS	0.4617	1.7561	0.0010	1.3416
SVI	0.4610	1.7599	0.0011	1.3416

For the optimal values obtained with respect to the second objective (Table 8), it is evident that the solutions are realistic and show significant improvement over the reduced placement optimum case. Although none of the models achieve the maximum sequestration of 1.92 Tscf observed in the placement optimum case, all models reach approximately 1.76 Tscf, which is a substantial increase from the initial 1.4 Tscf.

Table 9: Results on the optimal cases according to the third objective function

	f_1	f_2 (Tscf)	f_3	f_4 (Billion €)
DKL	0.5025	1.0473	1.00	0.8861
Dropout	0.5025	1.0473	1.00	0.8861
Ensemble	0.5078	0.9958	1.00	0.8495
GP	0.4951	1.1386	1.00	0.9501
MCMC	0.5040	1.0327	1.00	0.8759
IBNN	0.5221	0.8836	1.00	0.7643
NUTS	0.5370	0.7811	1.00	0.6899
SVI	0.5490	0.7468	1.00	0.6697

For the results corresponding to the third objective, all models successfully reached the maximum possible value (Table 9). The underlying explanation is similar to what was observed for two models in Table 7: the injection rate never declines due to a high recycling rate. These cases are characterized by low injection rates and high production rates, with a very lenient gas production constraint. Consequently, despite continuous injection, both NPV and total sequestration remain low.

Table 10: Results on the optimal cases according to the fourth objective function

	f_1	f_2 (Tscf)	f_3	f_4 (Billion €)
DKL	0.4691	1.7506	0.0003	1.3611
Dropout	0.4701	1.7467	0.0004	1.3572
Ensemble	0.4677	1.7590	0.0004	1.3634
GP	0.4678	1.7605	0.0004	1.3651
MCMC	0.4696	1.7489	0.0004	1.3579
IBNN	0.4693	1.7469	0.0004	1.3556
NUTS	0.4698	1.7463	0.0004	1.3561
SVI	0.4695	1.7452	0.0004	1.3562

Similarly to the second objective, the best solutions for the fourth objective (Table 10) exhibit a more conventional behavior compared to those of the first and third objectives. The NPV values increase by 200 million € relative to the benchmark reduced placement optimum case. Although the NPV remains lower than that of the placement optimum case, the trade-off between achieving a lower NPV with only three wells drilled versus a higher NPV with eight wells drilled can be justified more convincingly.

Notably, by comparing the best solutions obtained for the second and fourth objectives, a key distinction emerges: in the latter case, the injection rate declines more rapidly due to reduced brine production, as it incurs additional costs. In contrast, for the second objective, the injection rate typically decreases more gradually since brine withdrawal is not a limiting factor. This distinction highlights that while both cases yield similar solutions in terms of overall performance, their solution profiles differ significantly, aligning with the priorities of their respective optimization objectives.

This concludes the comparison between the optimized solutions and the benchmark cases. Moving forward, the focus shifts to evaluating the quality of solutions across individual objectives and assessing the overall improvement in terms of hypervolume. The following plots illustrate the progression of optimal objective values identified for each model as a function of the number of objective evaluations. Since each model was tested across eight trials, the average performance at each step is represented by dashed lines, while the range between the maximum and minimum values is shaded using the same color as the corresponding line.

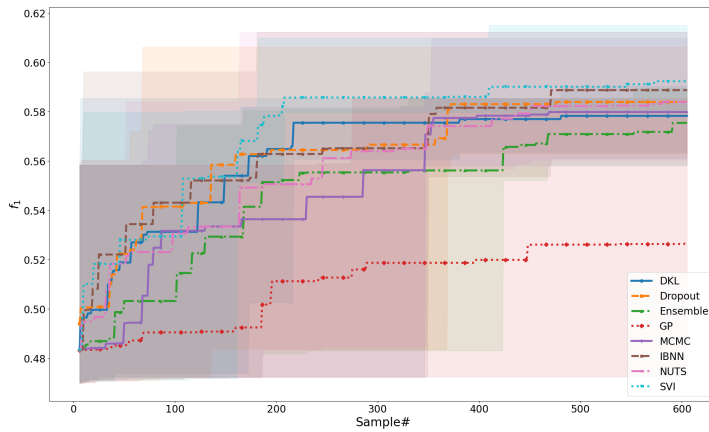


Figure 10: Maximum objective function value vs iteration number

In Figure 10, the evaluation results for f_1 are presented. While most models converge on average to a similar optimal value, the GP model exhibits significantly lower average values. This discrepancy can be partially explained by the shaded region, which represents the range of values encountered across trials. The broad spread for GP suggests that in at least one trial, the model never approached the optimal value of the first objective, leading to consistently lower performance. On average and on the maximum case, SVI models found the most optimal values for the first objective, followed by IBNN and Dropout.

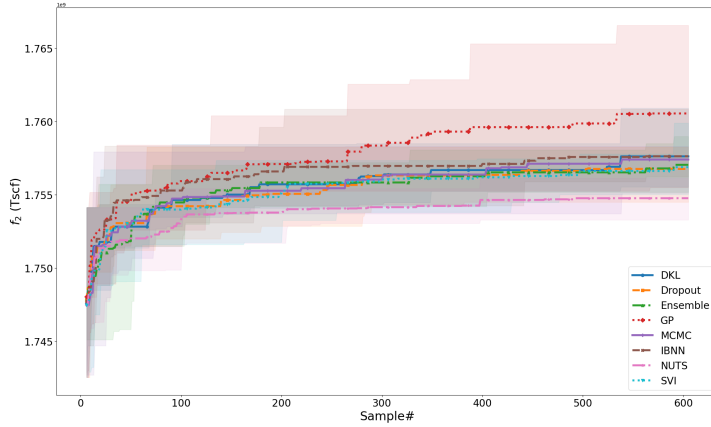


Figure 11: Maximum objective function value vs iteration number

In Figure 11, the results for the total sequestration volume f_2 are presented. This is one of the most critical objective functions, as it is commonly used to assess the success of a CCS project in its most simplified form, without considering economic, contractual, or safety constraints. Most models demonstrate a sharp initial improvement in their predictions, followed by a more gradual refinement over time. On average, the performance of most models is comparable; however, the GP model achieves the highest average results, consistently outperforming the others in maximizing total sequestration. In contrast, the NUTS model exhibits the lowest average performance, with a noticeably slower convergence towards higher sequestration volumes. The spread of shaded regions further indicates that the variability across trials is relatively limited for most models, suggesting stable performance trends.

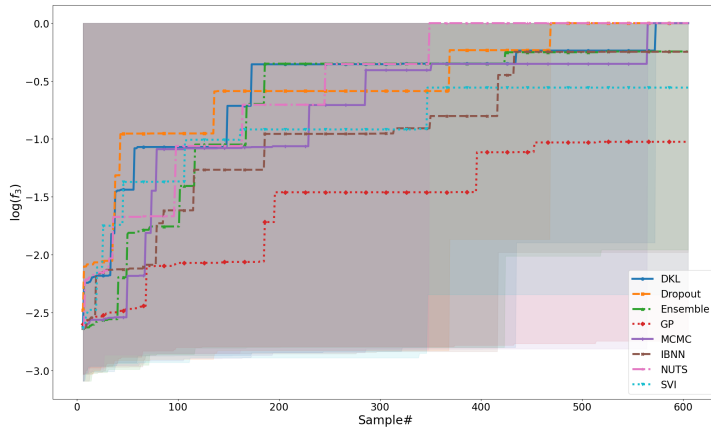


Figure 12: Maximum objective function value vs iteration number

The penalty function f_3 's results are presented in Figure 12 in logarithmic scale. The wide shaded areas indicate that in at least one trial, every model was able to reach the maximum possible value for the third objective. Notably, the NUTS, MCMC and DKL models consistently

found such solutions across all trials, whereas the GP model exhibited the lowest overall average performance. The presence of shaded regions near the value of -3 suggests that in many trials, some models never explored solutions that maximize the third objective. In general, values greater than -2 for this objective correspond to unconventional solutions characterized by high recycling rates. This explains the large variability observed in the shaded regions of the plot, reflecting the distinct exploration strategies adopted by different models across various trials.

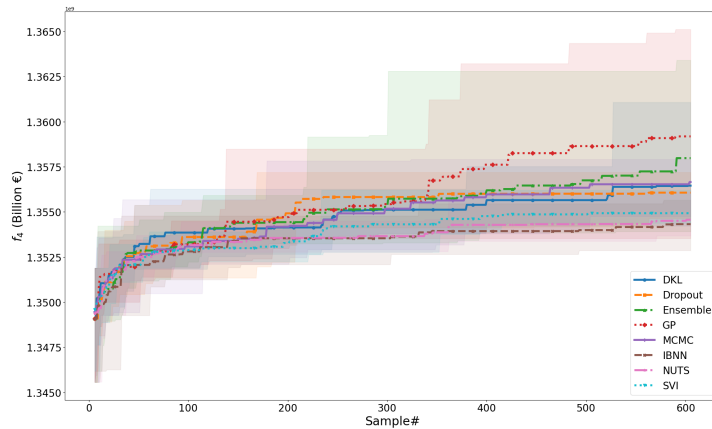


Figure 13: Maximum objective function value vs iteration number

Results for the f_4 (NPV) value are shown in Figure 13. This is the most critical objective in a CCS project, as it ultimately determines whether stakeholders choose to proceed with the operation. The NPV used in this analysis is simplified, as drilling costs were omitted and operational pricing was based on speculative estimates. However, this level of simplification remains sufficient for the scope of this work, as the variables optimized do not necessitate greater economic complexity. Once again, the GP model demonstrates the best average performance, followed by the Ensemble model. The convergence pattern across all models follows a typical trend: a rapid initial increase, followed by a more gradual improvement in later iterations. However, this gradual increase appears more pronounced compared to the results in Figure 11, which corresponds to the second objective function (total sequestration). This suggests that optimizing for NPV requires a more extended search process before stabilizing at near-optimal values.

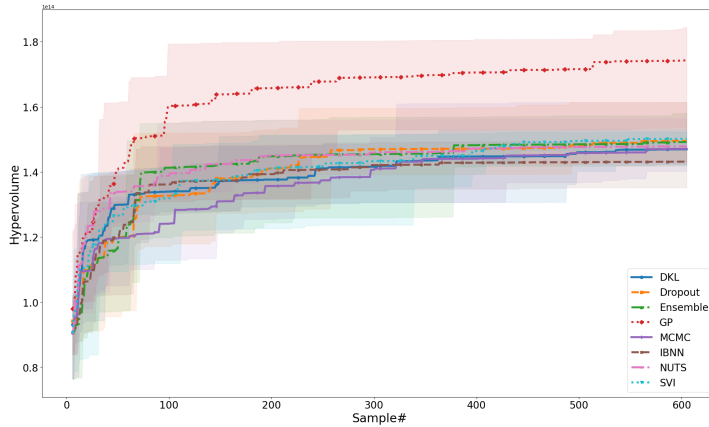


Figure 14: Hypervolume vs iteration number

Figure 14 presents the evolution of the hypervolume measure at each iteration, representing the hypervolume of the current set of all non-dominated solutions found up to that point. The characteristic behavior of hypervolume curves is evident: an initially low value, followed by a rapid increase in early iterations and eventually a plateau where improvements become marginal. Among all models, GP demonstrated the best overall performance, both in terms of average hypervolume and maximum values reached. In contrast, all other models plateau at significantly lower values. Regarding convergence speed, GP, Ensemble and NUTS converge more rapidly, whereas Dropout, MCMC and DKL exhibit slower convergence on average.

5. Discussion

In this work, the applicability of BNNs for CO₂ storage optimization has been investigated. At a high level, the optimization results achieved can be interpreted as very successful. In Case study 1, by simply optimizing the rates without adding any sort of extra operational cost, the operator is now able to steadily inject the target amount of CO₂ resulting in much higher total sequestration than the benchmark case. In Case study 2, by aggregating 6 producing wells into one, thus saving field development costs, the optimizer was able to sequester up to 91% of the CO₂ mass achieved in the benchmark case, although the total CO₂ mass sequestered accounted for only one of the four objective functions. Similarly, the optimal NPV computed for most models was as high as 92% of the benchmark, despite the fact that five less wells were utilized in the injection phase.

This high level evaluation is only the tip of the iceberg of the goals set by this research work. The most important and most difficult is to compare the ability of the various stochastic models to act as suitable surrogate models for BO. GPs are often used as the default approach due to ease of implementation and ability to be customized by a kernel function to shape the posterior probability distribution as needed. BNNs constitute an attractive alternative not hindered by the limitations of GPs such as high dimensional spaces and translation invariance of the kernel functions most commonly applied. In this work however, no discernible improvement was noticed by utilizing alternative models. On a positive note, their performance was comparable to GPs in

most cases and outperformed them at times. In Case study 1, GPs were expected to outperform BNNs due to the small number of decision variables. GPs proved able to only find more improvements in the objective function than BNNs in the second variation of Case study 1 but not in the first. Furthermore, they were never able to clearly outperform BNNs in terms of finding a better overall optimum. On the other hand, in Case study 2, BNNs were expected to take the upper hand due to the large increase in decision variables and the use of multiple objectives with completely different scales. Unexpectedly, GPs were shown to overperform the BNN surrogates.

On another note, it is important to question whether or not utilizing approximate rather than exact Bayesian inference is preferable when incorporated to neural networks. The NUTS and SVI models training took much more time than other methods due to a more intricate sampling process. However, their performance proved to be similar to that of approximate Bayesian methods such as Dropout, Ensemble and DKL. Despite being more robust, this did not translate into creating better performing surrogates. Nevertheless, this analysis is not fully comprehensive as the models are very sensitive to the choice of the hyperparameters. Consequently, concrete results cannot be obtained unless a detailed analysis is run on the selection of the hyperparameter values.

Another important reason for the models not exhibiting pronounced differences in their performance is the high non-linearity between the decision variables and the objective function output. The decision variables utilized in the optimization process are the rates that each well or group is targeted to produce/inject, not necessarily the ones that will actually be implemented. For example, when a well is set to operate at a production rate such that the bottom hole pressure limit is reached early, the control policy will force the actual production to significantly drop giving a non-linear response to the objective function. This shouldn't be a problem for the surrogates in this work as they are capable of coping with non-linearity. Non-linearity however is enhanced not only to bottom hole pressure constraints but also to acceptable CO₂ recycling rate constraint as well as the combined effects that other impose on its performance. The non-linearity may be further enhanced to the point of no correlation at all between the decision variables and the observed output. This is much more strongly demonstrated in Case study 2, where the decision variables at the later time steps are very sensitive to the selection of the decision variables at earlier time steps when it comes to their effect on the system response. Nevertheless, it should be noted that, apart from the performance of the optimization methods, this behavior is a direct result of the aquifer being a small and synthetic static model in comparison to areally extended ones typically considered in CCS operations.

6. Conclusions

BO is a very exciting avenue for reservoir engineering operations and management optimization which has not yet been adequately explored. Following the work of Li [80] it has been much easier recently to apply BO and even evaluate the performance of various robust BNN surrogates. Research in BO has started to take off recently and this work presents one of the first attempts in the reservoir engineering scientific area where BO has been implemented to optimize decision variables in a CCS operation. BO proved to be a very powerful process in the single as well as the multi-objective and many decision variables cases, that CCS projects usually constitute. It was shown to provide realistic solutions and greatly improve on the benchmark reduced placement optimum case. Most importantly, the NPV demonstrated a very significant improvement. The NPV can be the metric that makes or breaks a CCS project, as it can give the initial incentive to

operators and stakeholders to take up a project and allocate resources towards it.

Useful results were taken on the surrogate models' ability to find optimal values despite the limitations of the framework discussed in Section 5. Avenues for further research are available following this work. Detecting decision variables that better correlate to output performance, utilizing larger models for better correlation of system response and decision variables, combining well placement and well rates as decision variables simultaneously, adding models of larger complexity and more detailed geomechanical constraints and last but not least, utilizing optimization algorithms in a closed loop setting possibly by Reinforcement Learning [137] algorithms that provide very suitable frameworks for this task.

Credit author statement

Conceptualization, S.F. and V.G.; methodology, S.F.; software, S.F.; validation, S.F. and V.G.; resources, S.F.; writing—original draft preparation, S.F.; writing—review and editing, S.F., V.G.; visualization, S.F. All authors have read and agreed to the final version of the manuscript.

Declaration of competing interest

The authors declare that they have no known competing financial interests or personal relationships that could have appeared to influence the work reported in this paper.

Funding

The resources were granted with the support of GRNET as part of the project StorageCO₂.

References

- [1] S. M. Jarvis, S. Samsatli, Technologies and infrastructures underpinning future co2 value chains: A comprehensive review and comparative analysis, *Renewable and Sustainable Energy Reviews* 85 (2018) 46–68.
- [2] P. Gabrielli, M. Gazzani, M. Mazzotti, The role of carbon capture and utilization, carbon capture and storage, and biomass to enable a net-zero-co2 emissions chemical industry, *Industrial & Engineering Chemistry Research* 59 (15) (2020) 7033–7045.
- [3] M. Bui, G. D. Puxty, M. Gazzani, S. M. Soltani, C. Pozo, The role of carbon capture and storage (ccs) technologies in a net-zero carbon future (2021).
- [4] S. Rackley, S. Rackley, Introduction to geological storage, *Carbon Capture and Storage*; Elsevier: Amsterdam, The Netherlands (2017) 285–304.
- [5] L. Tomić, V. K. Maričić, D. Danilović, M. Crnogorac, Criteria for co2 storage in geological formations, *Podzemni radovi* (32) (2018) 61–74.
- [6] X. Ji, C. Zhu, Co2 storage in deep saline aquifers, in: *Novel materials for carbon dioxide mitigation technology*, Elsevier, 2015, pp. 299–332.
- [7] S. Bachu, Review of co2 storage efficiency in deep saline aquifers, *International Journal of Greenhouse Gas Control* 40 (2015) 188–202.
- [8] K. Michael, A. Golab, V. Shulakova, J. Ennis-King, G. Allinson, S. Sharma, T. Aiken, Geological storage of co2 in saline aquifers—a review of the experience from existing storage operations, *International journal of greenhouse gas control* 4 (4) (2010) 659–667.
- [9] S. Hannis, J. Lu, A. Chadwick, S. Hovorka, K. Kirk, K. Romanak, J. Pearce, Co2 storage in depleted or depleting oil and gas fields: what can we learn from existing projects?, *Energy Procedia* 114 (2017) 5680–5690.
- [10] E. Mohammadian, B. M. Jan, A. Azdarpour, H. Hamidi, N. H. B. Othman, A. Dollah, S. N. B. C. M. Hussein, R. A. B. Sazali, Co 2-eor/sequestration: Current trends and future horizons, in: *Enhanced Oil Recovery Processes-New Technologies*, IntechOpen, 2019.
- [11] Z. Li, M. Dong, S. Li, S. Huang, Co2 sequestration in depleted oil and gas reservoirs—caprock characterization and storage capacity, *Energy Conversion and Management* 47 (11-12) (2006) 1372–1382.
- [12] I. Ismail, V. Gaganis, Carbon capture, utilization, and storage in saline aquifers: Subsurface policies, development plans, well control strategies and optimization approaches—a review, *Clean Technologies* 5 (2) (2023) 609–637.
- [13] K. Pruess, J. García, T. Kovscek, C. Oldenburg, J. Rutqvist, C. Steefel, T. Xu, Code intercomparison builds confidence in numerical simulation models for geologic disposal of co2, *Energy* 29 (9-10) (2004) 1431–1444.
- [14] H. Class, A. Ebigbo, R. Helmig, H. K. Dahle, J. M. Nordbotten, M. A. Celia, P. Audigane, M. Darcis, J. Ennis-King, Y. Fan, et al., A benchmark study on problems related to co 2 storage in geologic formations: summary and discussion of the results, *Computational geosciences* 13 (2009) 409–434.
- [15] S. Whitaker, Flow in porous media i: A theoretical derivation of darcy’s law, *Transport in porous media* 1 (1986) 3–25.
- [16] A. F. Rasmussen, T. H. Sandve, K. Bao, A. Lauser, J. Hove, B. Skaflestad, R. Klöfkorn, M. Blatt, A. B. Rustad, O. Sævareid, et al., The open porous media flow reservoir simulator, *Computers & Mathematics with Applications* 81 (2021) 159–185.
- [17] J. A. Trangenstein, J. B. Bell, Mathematical structure of the black-oil model for petroleum reservoir simulation, *SIAM Journal on Applied Mathematics* 49 (3) (1989) 749–783.
- [18] A. Cihan, J. T. Birkholzer, M. Bianchi, Optimal well placement and brine extraction for pressure management during co2 sequestration, *International Journal of Greenhouse Gas Control* 42 (2015) 175–187.
- [19] D. A. Cameron, L. J. Durlofsky, Optimization of well placement, co2 injection rates, and brine cycling for geological carbon sequestration, *International Journal of Greenhouse Gas Control* 10 (2012) 100–112.
- [20] S. Bachu, Co2 storage in geological media: Role, means, status and barriers to deployment, *Progress in energy and combustion science* 34 (2) (2008) 254–273.
- [21] H. De Coninck, T. Flach, P. Curnow, P. Richardson, J. Anderson, S. Shackley, G. Sigurthorsson, D. Reiner, The acceptability of co2 capture and storage (ccs) in europe: An assessment of the key determining factors: Part 1. scientific, technical and economic dimensions, *International Journal of Greenhouse Gas Control* 3 (3) (2009) 333–343.
- [22] K. W. Bandilla, M. A. Celia, Active pressure management through brine production for basin-wide deployment of geologic carbon sequestration, *International Journal of Greenhouse Gas Control* 61 (2017) 155–167.
- [23] T. A. Buscheck, J. M. Bielicki, J. A. White, Y. Sun, Y. Hao, W. L. Bourcier, S. A. Carroll, R. D. Aines, Pre-injection brine production in co2 storage reservoirs: An approach to augment the development, operation, and performance of ccs while generating water, *International Journal of Greenhouse Gas Control* 54 (2016) 499–512.
- [24] S. T. Anderson, H. Jahediesfanjani, Estimating the net costs of brine production and disposal to expand pressure-limited dynamic capacity for basin-scale co2 storage in a saline formation, *International Journal of Greenhouse Gas Control* 102 (2020) 103161.

- [25] Y. Wang, Y. Xu, K. Zhang, Investigation of co2 storage capacity in open saline aquifers with numerical models, *Procedia Engineering* 31 (2012) 886–892.
- [26] K. Deb, K. Sindhya, J. Hakanen, Multi-objective optimization, in: *Decision sciences*, CRC Press, 2016, pp. 161–200.
- [27] S. Mirjalili, S. Mirjalili, Genetic algorithm, *Evolutionary Algorithms and Neural Networks: Theory and Applications* (2019) 43–55.
- [28] J. Kennedy, R. Eberhart, Particle swarm optimization, in: *Proceedings of ICNN'95-international conference on neural networks*, Vol. 4, IEEE, 1995, pp. 1942–1948.
- [29] B. Guyaguler, R. N. Horne, L. Rogers, J. J. Rosenzweig, Optimization of well placement in a gulf of mexico waterflooding project, *SPE Reservoir Evaluation & Engineering* 5 (03) (2002) 229–236.
- [30] T. A. El-Mihoub, A. A. Hopgood, L. Nolle, A. Battersby, Hybrid genetic algorithms: A review., *Eng. Lett.* 13 (2) (2006) 124–137.
- [31] O. Badru, C. Kabir, Well placement optimization in field development, in: *SPE Annual Technical Conference and Exhibition, OnePetro*, 2003.
- [32] A. A. Emerick, E. Silva, B. Messer, L. F. Almeida, D. Szwarcman, M. A. C. Pacheco, M. M. Vellasco, Well placement optimization using a genetic algorithm with nonlinear constraints, in: *SPE Reservoir Simulation Conference?*, SPE, 2009, pp. SPE–118808.
- [33] Z. Michalewicz, G. Nazhiyath, Genocop iii: A co-evolutionary algorithm for numerical optimization problems with nonlinear constraints, in: *Proceedings of 1995 IEEE International Conference on Evolutionary Computation*, Vol. 2, IEEE, 1995, pp. 647–651.
- [34] J. Stopa, D. Janiga, P. Wojnarowski, R. Czarnota, Optimization of well placement and control to maximize co2 trapping during geologic sequestration, *AGH Drilling, Oil, Gas* 33 (1) (2016) 93–104.
- [35] T. Goda, K. Sato, Global optimization of injection well placement toward higher safety of co2 geological storage, *Energy Procedia* 37 (2013) 4583–4590.
- [36] W.-L. Loh, On latin hypercube sampling, *The annals of statistics* 24 (5) (1996) 2058–2080.
- [37] J. Hutahaean, V. Demyanov, D. Arnold, O. Vazquez, Optimization of well placement to minimize the risk of scale deposition in field development, in: *Abu Dhabi international petroleum exhibition and conference*, SPE, 2014, p. D021S026R002.
- [38] J. Islam, P. M. Vasant, B. M. Negash, M. B. Laruccia, M. Myint, J. Watada, A holistic review on artificial intelligence techniques for well placement optimization problem, *Advances in engineering software* 141 (2020) 102767.
- [39] A. Cozad, N. V. Sahinidis, D. C. Miller, Learning surrogate models for simulation-based optimization, *AICHE Journal* 60 (6) (2014) 2211–2227.
- [40] Y. S. Ong, P. B. Nair, A. J. Keane, Evolutionary optimization of computationally expensive problems via surrogate modeling, *AIAA journal* 41 (4) (2003) 687–696.
- [41] Y. Jin, Surrogate-assisted evolutionary computation: Recent advances and future challenges, *Swarm and Evolutionary Computation* 1 (2) (2011) 61–70.
- [42] M. Babaei, I. Pan, Performance comparison of several response surface surrogate models and ensemble methods for water injection optimization under uncertainty, *Computers & Geosciences* 91 (2016) 19–32.
- [43] T. Goel, R. T. Haftka, W. Shyy, N. V. Queipo, Ensemble of surrogates, *Structural and Multidisciplinary Optimization* 33 (2007) 199–216.
- [44] E. Santibanez-Borda, R. Govindan, N. Elahi, A. Korre, S. Durucan, Maximising the dynamic co2 storage capacity through the optimisation of co2 injection and brine production rates, *International Journal of Greenhouse Gas Control* 80 (2019) 76–95.
- [45] B. Amiri, A. Jahanbani Ghahfarokhi, V. Rocca, C. S. W. Ng, Optimization of offshore saline aquifer co2 storage in smeaheia using surrogate reservoir models, *Algorithms* 17 (10) (2024). doi:10.3390/a17100452. URL <https://www.mdpi.com/1999-4893/17/10/452>
- [46] C. Szegedy, W. Zaremba, I. Sutskever, J. Bruna, D. Erhan, I. Goodfellow, R. Fergus, Intriguing properties of neural networks, *arXiv preprint arXiv:1312.6199* (2013).
- [47] C. Guo, G. Pleiss, Y. Sun, K. Q. Weinberger, On calibration of modern neural networks, in: *International conference on machine learning*, PMLR, 2017, pp. 1321–1330.
- [48] J. Nixon, M. W. Dusenberry, L. Zhang, G. Jerfel, D. Tran, Measuring calibration in deep learning., in: *CVPR workshops*, Vol. 2, 2019.
- [49] P. I. Frazier, A tutorial on bayesian optimization, *arXiv preprint arXiv:1807.02811* (2018).
- [50] A. Der Kiureghian, O. Ditlevsen, Aleatory or epistemic? does it matter?, *Structural safety* 31 (2) (2009) 105–112.
- [51] E. Hüllermeier, W. Waegeman, Aleatoric and epistemic uncertainty in machine learning: An introduction to concepts and methods, *Machine learning* 110 (3) (2021) 457–506.
- [52] R. J. Adler, *An introduction to continuity, extrema, and related topics for general gaussian processes*, IMS, 1990.
- [53] K. Balabaeva, L. Akmadieva, S. Kovalchuk, Optimal wells placement to maximize the field cov-

- erage using derivative-free optimization, *Procedia Computer Science* 178 (2020) 65–74, 9th International Young Scientists Conference in Computational Science, YSC2020, 05-12 September 2020. doi:<https://doi.org/10.1016/j.procs.2020.11.008>. URL <https://www.sciencedirect.com/science/article/pii/S1877050920323814>
- [54] R. Bordas, J. Heritage, M. Javed, G. Peacock, T. Taha, P. Ward, I. Vernon, R. Hammersley, A bayesian optimisation workflow for field development planning under geological uncertainty, in: *ECMOR XVII*, Vol. 2020, European Association of Geoscientists & Engineers, 2020, pp. 1–20.
- [55] A. Kumar, Search space partitioning, mcts and trust-region bayesian optimization for joint optimization of well placement and control, in: *83rd EAGE Annual Conference & Exhibition*, Vol. 2022, European Association of Geoscientists & Engineers, 2022, pp. 1–5.
- [56] A. Kumar, High-dimensional bayesian optimization using sparse-axis aligned subspaces for joint optimization of well control and placement, in: *84th EAGE Annual Conference & Exhibition*, Vol. 2023, European Association of Geoscientists & Engineers, 2023, pp. 1–5.
- [57] D. Eriksson, M. Pearce, J. Gardner, R. D. Turner, M. Poloczek, Scalable global optimization via local bayesian optimization, *Advances in neural information processing systems* 32 (2019).
- [58] D. Eriksson, M. Jankowiak, High-dimensional bayesian optimization with sparse axis-aligned subspaces, in: *Uncertainty in Artificial Intelligence*, PMLR, 2021, pp. 493–503.
- [59] X. Lu, K. E. Jordan, M. F. Wheeler, E. O. Pyzer-Knapp, M. Benatan, Bayesian optimization for field-scale geological carbon storage, *Engineering* 18 (2022) 96–104. doi:<https://doi.org/10.1016/j.eng.2022.06.011>. URL <https://www.sciencedirect.com/science/article/pii/S2095809922004957>
- [60] M. A. Javed, Bayesian optimization of deviated well trajectories under geological uncertainty, MSc thesis for Heriot-Watt University (2020).
- [61] S. Wang, S. Chen, A novel bayesian optimization framework for computationally expensive optimization problem in tight oil reservoirs, in: *SPE Annual Technical Conference and Exhibition?*, SPE, 2017, p. D021S014R007.
- [62] Z. Wang, S. Jegelka, Max-value entropy search for efficient bayesian optimization, in: *International Conference on Machine Learning*, PMLR, 2017, pp. 3627–3635.
- [63] J. Gardner, C. Guo, K. Weinberger, R. Garnett, R. Grosse, Discovering and exploiting additive structure for bayesian optimization, in: *Artificial Intelligence and Statistics*, PMLR, 2017, pp. 1311–1319.
- [64] K. Kandasamy, J. Schneider, B. Póczos, High dimensional bayesian optimisation and bandits via additive models, in: *International conference on machine learning*, PMLR, 2015, pp. 295–304.
- [65] J. Wu, M. Poloczek, A. G. Wilson, P. Frazier, Bayesian optimization with gradients, *Advances in neural information processing systems* 30 (2017).
- [66] K. Swersky, J. Snoek, R. P. Adams, Multi-task bayesian optimization, *Advances in neural information processing systems* 26 (2013).
- [67] H. Moss, D. Leslie, D. Beck, J. Gonzalez, P. Rayson, Boss: Bayesian optimization over string spaces, *Advances in neural information processing systems* 33 (2020) 15476–15486.
- [68] R. Garnett, *Bayesian optimization*, Cambridge University Press, 2023.
- [69] S. P. Fotias, I. Ismail, V. Gaganis, Optimization of well placement in carbon capture and storage (ccs): Bayesian optimization framework under permutation invariance, *Applied Sciences* 14 (8) (2024) 3528.
- [70] T. Buckle, R. Hutton, V. Demyanov, D. Arnold, A. Antropov, E. Kharyba, M. Pilipenko, L. Stulov, Improving local history match using machine learning generated regions from production response and geological parameter correlations, in: *Petroleum Geostatistics 2019*, Vol. 2019, European Association of Geoscientists & Engineers, 2019, pp. 1–5.
- [71] D. Arnold, V. Demyanov, M. Christie, A. Bakay, K. Gopa, Optimisation of decision making under uncertainty throughout field lifetime: A fractured reservoir example, *Computers & Geosciences* 95 (2016) 123–139.
- [72] M. Sambridge, Geophysical inversion with a neighbourhood algorithm—i. searching a parameter space, *Geophysical journal international* 138 (2) (1999) 479–494.
- [73] M. Sambridge, Geophysical inversion with a neighbourhood algorithm—ii. appraising the ensemble, *Geophysical Journal International* 138 (3) (1999) 727–746.
- [74] J. Hutahaean, V. Demyanov, M. Christie, Reservoir development optimization under uncertainty for infill well placement in brownfield redevelopment, *Journal of Petroleum Science and Engineering* 175 (2019) 444–464.
- [75] L. Mohamed, M. Christie, V. Demyanov, Comparison of stochastic sampling algorithms for uncertainty quantification, *SPE journal* 15 (01) (2010) 31–38.
- [76] Q. Liao, L. Zeng, H. Chang, D. Zhang, Efficient history matching using the markov-chain monte carlo method by means of the transformed adaptive stochastic collocation method, *SPE Journal* 24 (04) (2019) 1468–1489.
- [77] X. Ma, M. Al-Harbi, A. Datta-Gupta, Y. Efendiev, An efficient two-stage sampling method for uncertainty quantification in history matching geological models, *SPE Journal* 13 (01) (2008) 77–87.
- [78] F. Olalotiti-Lawal, A. Datta-Gupta, A multiobjective markov chain monte carlo approach for history matching and uncertainty quantification, *Journal of Petroleum Science and Engineering* 166 (2018) 759–777.

- [79] R. M. Neal, Bayesian learning for neural networks, Vol. 118, Springer Science & Business Media, 2012.
- [80] Y. L. Li, T. G. Rudner, A. G. Wilson, A study of bayesian neural network surrogates for bayesian optimization, arXiv preprint arXiv:2305.20028 (2023).
- [81] M. Balandat, B. Karrer, D. Jiang, S. Daulton, B. Letham, A. G. Wilson, E. Bakshy, Botorch: A framework for efficient monte-carlo bayesian optimization, *Advances in neural information processing systems* 33 (2020) 21524–21538.
- [82] J. E. Onwunali, L. J. Durlofsky, Application of a particle swarm optimization algorithm for determining optimum well location and type, *Computational Geosciences* 14 (2010) 183–198.
- [83] C. K. Williams, C. E. Rasmussen, Gaussian processes for machine learning, Vol. 2, MIT press Cambridge, MA, 2006.
- [84] Z. Dou, Bayesian global optimization approach to the oil well placement problem with quantified uncertainties, Ph.D. thesis, Purdue University (2015).
- [85] A. Agnihotri, N. Batra, Exploring bayesian optimization, *Distill* 5 (5) (2020) e26.
- [86] J. Görtler, R. Kehlbeck, O. Deussen, A visual exploration of gaussian processes, *Distill* 4 (4) (2019) e17.
- [87] C. B. Do, The multivariate gaussian distribution, Section Notes, Lecture on Machine Learning, CS 229 (2008).
- [88] M. G. Genton, Classes of kernels for machine learning: a statistics perspective, *Journal of machine learning research* 2 (Dec) (2001) 299–312.
- [89] F. W. Olver, L. C. Maximon, Bessel functions. (2010).
- [90] E. Artin, The gamma function, Courier Dover Publications, 2015.
- [91] E. Goan, C. Fookes, Bayesian neural networks: An introduction and survey, *Case Studies in Applied Bayesian Data Science: CIRM Jean-Morlet Chair, Fall 2018* (2020) 45–87.
- [92] D. M. Titterton, Bayesian methods for neural networks and related models, *Statistical science* (2004) 128–139.
- [93] J. Lampinen, A. Vehtari, Bayesian approach for neural networks—review and case studies, *Neural networks* 14 (3) (2001) 257–274.
- [94] L. V. Jospin, H. Laga, F. Boussaid, W. Buntine, M. Bennamoun, Hands-on bayesian neural networks—a tutorial for deep learning users, *IEEE Computational Intelligence Magazine* 17 (2) (2022) 29–48.
- [95] Z.-H. Zhou, Ensemble methods: foundations and algorithms, CRC press, 2012.
- [96] D. J. MacKay, A practical bayesian framework for backpropagation networks, *Neural computation* 4 (3) (1992) 448–472.
- [97] P. J. Werbos, Backpropagation through time: what it does and how to do it, *Proceedings of the IEEE* 78 (10) (1990) 1550–1560.
- [98] P. Izmailov, S. Vikram, M. D. Hoffman, A. G. G. Wilson, What are bayesian neural network posteriors really like?, in: *International conference on machine learning*, PMLR, 2021, pp. 4629–4640.
- [99] W. K. Hastings, Monte carlo sampling methods using markov chains and their applications (1970).
- [100] W. R. Gilks, S. Richardson, D. Spiegelhalter, Markov chain Monte Carlo in practice, CRC press, 1995.
- [101] D. M. Blei, A. Kucukelbir, J. D. McAuliffe, Variational inference: A review for statisticians, *Journal of the American statistical Association* 112 (518) (2017) 859–877.
- [102] S. Kullback, R. A. Leibler, On information and sufficiency, *The annals of mathematical statistics* 22 (1) (1951) 79–86.
- [103] C. E. Shannon, A mathematical theory of communication, *The Bell system technical journal* 27 (3) (1948) 379–423.
- [104] M. D. Hoffman, D. M. Blei, C. Wang, J. Paisley, Stochastic variational inference, *Journal of Machine Learning Research* (2013).
- [105] A. Graves, Practical variational inference for neural networks, *Advances in neural information processing systems* 24 (2011).
- [106] H. Ritter, A. Botev, D. Barber, A scalable laplace approximation for neural networks, in: *6th international conference on learning representations, ICLR 2018-conference track proceedings*, Vol. 6, International Conference on Representation Learning, 2018.
- [107] W. J. Maddox, P. Izmailov, T. Garipov, D. P. Vetrov, A. G. Wilson, A simple baseline for bayesian uncertainty in deep learning, *Advances in neural information processing systems* 32 (2019).
- [108] J. M. Hernández-Lobato, R. Adams, Probabilistic backpropagation for scalable learning of bayesian neural networks, in: *International conference on machine learning*, PMLR, 2015, pp. 1861–1869.
- [109] C. Blundell, J. Cornebise, K. Kavukcuoglu, D. Wierstra, Weight uncertainty in neural network, in: *International conference on machine learning*, PMLR, 2015, pp. 1613–1622.
- [110] D. P. Kingma, J. Ba, Adam: A method for stochastic optimization, arXiv preprint arXiv:1412.6980 (2014).
- [111] D. P. Kingma, M. Welling, et al., An introduction to variational autoencoders, *Foundations and Trends® in Machine Learning* 12 (4) (2019) 307–392.
- [112] A. Kucukelbir, D. Tran, R. Ranganath, A. Gelman, D. M. Blei, Automatic differentiation variational inference, *Journal of machine learning research* 18 (14) (2017) 1–45.

- [113] R. M. Neal, Slice sampling, *The annals of statistics* 31 (3) (2003) 705–767.
- [114] R. Bardenet, A. Doucet, C. Holmes, On markov chain monte carlo methods for tall data, *Journal of Machine Learning Research* 18 (47) (2017) 1–43.
- [115] J. R. Norris, *Markov chains*, no. 2, Cambridge university press, 1998.
- [116] S. Chib, E. Greenberg, Understanding the metropolis-hastings algorithm, *The american statistician* 49 (4) (1995) 327–335.
- [117] M. Betancourt, A conceptual introduction to hamiltonian monte carlo, arXiv preprint arXiv:1701.02434 (2017).
- [118] R. M. Neal, Mcmc using hamiltonian dynamics, arXiv preprint arXiv:1206.1901 (2012).
- [119] M. Girolami, B. Calderhead, Riemann manifold langevin and hamiltonian monte carlo methods, *Journal of the Royal Statistical Society Series B: Statistical Methodology* 73 (2) (2011) 123–214.
- [120] M. D. Hoffman, A. Gelman, et al., The no-u-turn sampler: adaptively setting path lengths in hamiltonian monte carlo., *J. Mach. Learn. Res.* 15 (1) (2014) 1593–1623.
- [121] B. Leimkuhler, S. Reich, Symplectic integration of constrained hamiltonian systems, *Mathematics of Computation* 63 (208) (1994) 589–605.
- [122] H. Yoshida, Recent progress in the theory and application of symplectic integrators, in: *Qualitative and Quantitative Behaviour of Planetary Systems: Proceedings of the Third Alexander von Humboldt Colloquium on Celestial Mechanics*, Springer, 1993, pp. 27–43.
- [123] N. Srivastava, G. Hinton, A. Krizhevsky, I. Sutskever, R. Salakhutdinov, Dropout: A simple way to prevent neural networks from overfitting, *Journal of Machine Learning Research* 15 (56) (2014) 1929–1958.
URL <http://jmlr.org/papers/v15/srivastava14a.html>
- [124] Y. Gal, Z. Ghahramani, Dropout as a bayesian approximation: Representing model uncertainty in deep learning, in: M. F. Balcan, K. Q. Weinberger (Eds.), *Proceedings of The 33rd International Conference on Machine Learning*, Vol. 48 of *Proceedings of Machine Learning Research*, PMLR, New York, New York, USA, 2016, pp. 1050–1059.
URL <https://proceedings.mlr.press/v48/gal16.html>
- [125] B. Lakshminarayanan, A. Pritzel, C. Blundell, Simple and scalable predictive uncertainty estimation using deep ensembles, *Advances in neural information processing systems* 30 (2017).
- [126] Y. Ovadia, E. Fertig, J. Ren, Z. Nado, D. Sculley, S. Nowozin, J. Dillon, B. Lakshminarayanan, J. Snoek, Can you trust your model’s uncertainty? evaluating predictive uncertainty under dataset shift, *Advances in neural information processing systems* 32 (2019).
- [127] R. M. Neal, R. M. Neal, Priors for infinite networks, *Bayesian learning for neural networks* (1996) 29–53.
- [128] C. Williams, Computing with infinite networks, *Advances in neural information processing systems* 9 (1996).
- [129] J. Lee, Y. Bahri, R. Novak, S. S. Schoenholz, J. Pennington, J. Sohl-Dickstein, Deep neural networks as gaussian processes, arXiv preprint arXiv:1711.00165 (2017).
- [130] A. G. Wilson, Z. Hu, R. Salakhutdinov, E. P. Xing, Deep kernel learning, in: *Artificial intelligence and statistics*, PMLR, 2016, pp. 370–378.
- [131] D. W. Peaceman, *Fundamentals of numerical reservoir simulation*, Elsevier, 2000.
- [132] J. R. Gardner, G. Pleiss, D. Bindel, K. Q. Weinberger, A. G. Wilson, Gpytorch: Blackbox matrix-matrix gaussian process inference with gpu acceleration, in: *Advances in Neural Information Processing Systems*, 2018.
- [133] E. Bingham, J. P. Chen, M. Jankowiak, F. Obermeyer, N. Pradhan, T. Karaletsos, R. Singh, P. A. Szerlip, P. Horsfall, N. D. Goodman, Pyro: Deep universal probabilistic programming, *J. Mach. Learn. Res.* 20 (2019) 28:1–28:6.
URL <http://jmlr.org/papers/v20/18-403.html>
- [134] Z. E. Platform, The costs of co2 capture, *Transport and Storage Postdemonstration CCS in the EU* (2011).
- [135] A. IEA, *World energy model documentation* (2019).
- [136] E. J. Sullivan, S. Chu, P. H. Stauffer, R. S. Middleton, R. J. Pawar, A method and cost model for treatment of water extracted during geologic co2 storage, *International Journal of Greenhouse Gas Control* 12 (2013) 372–381.
- [137] R. S. Sutton, A. G. Barto, *Reinforcement learning: An introduction*, MIT press, 2018.